

Crane control system using exoskeleton based on programmable logic technology

Ryszard Ziętek¹✉, Marcin Woźniak²

West Pomeranian University of Technology
17 Piastów Ave., 70-310 Szczecin, Poland
e-mail: ¹zr34367@zut.edu.pl, ²marcin.wozniak@zut.edu.pl
✉ corresponding author

Key words: master-slave control, field-programmable logic cascade regulation, mechatronic system, exoskeleton, crane, manipulator kinematics

Abstract

In this paper, a mini-crane control system using an exoskeleton based on programmable logic technology is presented. The first stage was to identify the parameters of the mini-crane and exoskeleton sub-assemblies. Then, individual crane and exoskeleton control subsystems were designed based on cascade regulation. The final stage was to connect these subsystems into the master-slave control system using the manipulator's kinematics equations. Parallel processing was used to minimize delays in the control system. Analysis of the results showed that the difference between the set and measured crane position was small.

Introduction

Systems that allow the remote control of machines are increasingly used in many areas. Remote control, in addition to diagnostic systems (Bejger, Chybowski & Gawdzińska, 2018; Bejger & Drzewieniecki, 2020) and simulators (Chybowski et al., 2015), increases the safety of a machine operator's work. The military industry was the first to use remote-controlled devices for the recognition and neutralization of hostile objects (Hsu, Murray & Cook, 2013) and explosives disposal (Narayanan & Reddy, 2015). Remotely-controlled devices have also been used to remove radioactive waste (Holliday et al., 1993). Cosmonautics has also used remote-controlled devices, which significantly reduced the repair costs of spacecraft and satellites (Siciliano & Khatib, 2016).

The use of remote-controlled devices in medicine has reduced the risk of surgery failure (Chang et al., 2017). Increasingly, victims of natural disasters are being searched for using remotely-controlled robots (Kawatsuma, Fukushima & Okada, 2012). An area

with a growing demand for remote-controlled devices is industries that use remote object manipulation or remote material processing (Siciliano & Khatib, 2016).

Various methods for controlling cranes are presented later in the article. The first method for the remote control of a crane was controlled with a remote control (Miądlicki & Pajor, 2015). The use of a remote control significantly simplified the construction of control systems, but this increased functionality increased their operational difficulty. Joysticks were also used to control cranes (Miądlicki & Pajor, 2015), in which changing the deflection of the joystick caused the crane to move accordingly. Changes in the joystick position were measured based on a change in resistance (resistance joysticks), voltage (strain gauge joysticks), or inductance.

Along with the development of liquid crystal displays, a new control method has appeared – control via a control panel (Miądlicki & Pajor, 2015) – which allows a crane's position to be set and its trajectory defined using a control panel. After the appearance of the first integrated circuit (ETHW,

2017), the development of control systems based on them began, which significantly accelerated the repair process. Increasing the functionality and processing speed of integrated circuits has enabled the construction of more complex control systems using virtual reality (Pajor et al., 2011), as well as exoskeletons (Herbin & Pajor, 2018; Herbin & Woźniak, 2019). In addition, increasing the processing speed has increased the reliability of control systems (Kozak, Gordon & Bejger 2016).

The development of integrated circuit manufacturing technology has contributed to the creation of ASICs dedicated to specific tasks and circuits enabling the determination of appropriate functionality, using basic logic elements, such as logical sum and logical product gates – programmable circuits (Elektronika Praktyczna, 2004). The next family is CPLD systems, which consist of many interconnected basic logic elements consisting of AND and OR gates.

The latest programmable circuits are FPGAs built from logic cells with different functionalities (Kaeslin, 2015). Basic logic cells consist of a certain number of flip-flops and LUTs. FPGAs are also equipped with cells dedicated to special tasks, such as cells used in digital signal processing (DSP) and block RAM cells. The operation of programmable systems is based on the configuration of the bits responsible for switching on the appropriate system cells (Kaeslin, 2015). The above action allows the design of applications based on parallel processing.

The control system presented in this paper increases the safety of the machine operator by enabling the crane to be controlled from a distance. By using the appropriate robot gripper, remote manipulation of objects is possible.

Experimental stand

The experimental stand (Figure 1) consists of a mechanical subsystem and an electronic subsystem. The mechanical subsystem consists of:

- An exoskeleton, whose task is to change the position of the exoskeleton's end effector under the influence of the exoskeleton operator and to transfer information about the displacement of the end effector to the control system.
- A mini-crane that moves the crane end effector by a value equal to the displacement of the exoskeleton end effector. It is a laboratory mini-crane designed to test control systems.

The electronic subsystem of the experimental stand consists of:

- A DS control and measuring board, whose task is to enable and supply analog signals to the appropriate actuators of the mechanical subsystem and to register signals generated on the measuring elements of the mechanical part of the experimental stand.
- A calculation board with an FPGA system on which the control system was implemented. The task of the computing board is also to properly process the data using the ADC converters on the board.

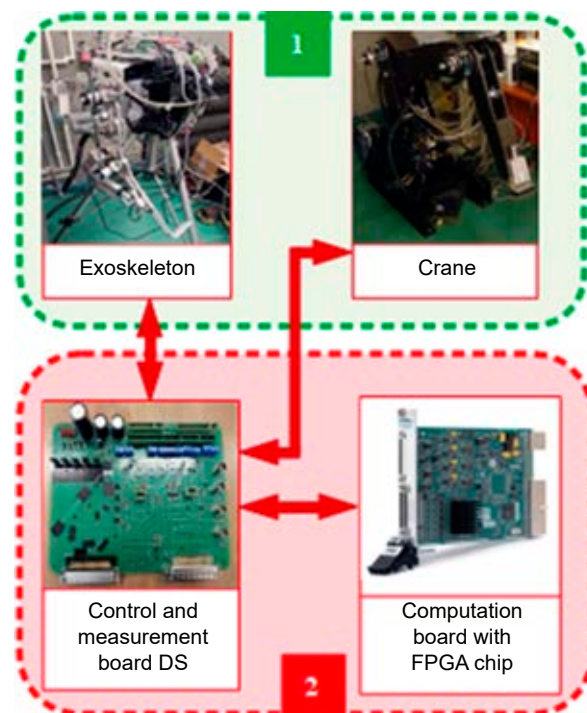


Figure 1. Experimental stand

The diagram of the kinematic structure is shown in Figure 2.

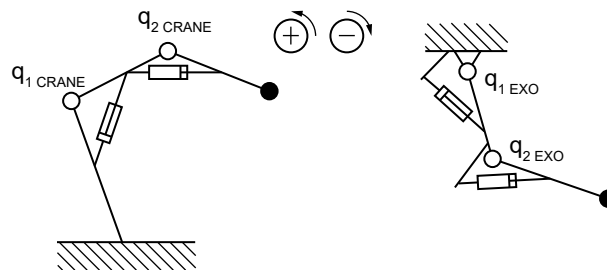


Figure 2. Diagram of the kinematic structure (Herbin & Woźniak, 2019)

Control system

Figure 3 shows the control system, which consists of an exoskeleton control subsystem (1) and a crane

control subsystem (2). The first step to change the position of the crane is to move the exoskeleton end effector. The operator acting on the effector changes the forces measured on the strain gauge beams of the individual exoskeleton members. These forces are then transmitted to the exoskeleton displacement regulator, which changes the position of the exoskeleton's effector, sending appropriate signals to the exoskeleton actuators. Information about changing the angular position of the exoskeleton joints is sent

to the crane control subsystem. The exoskeleton displacement regulator is based on signals from strain gauges.

The first component of the crane control subsystem is the crane displacement regulator (Figure 3), which consists of 3 parts:

- Exoskeleton displacement calculation section (Figure 4 – green section), which consists of a unit that implements forward kinematics equations that calculate the position of the exoskeleton's end

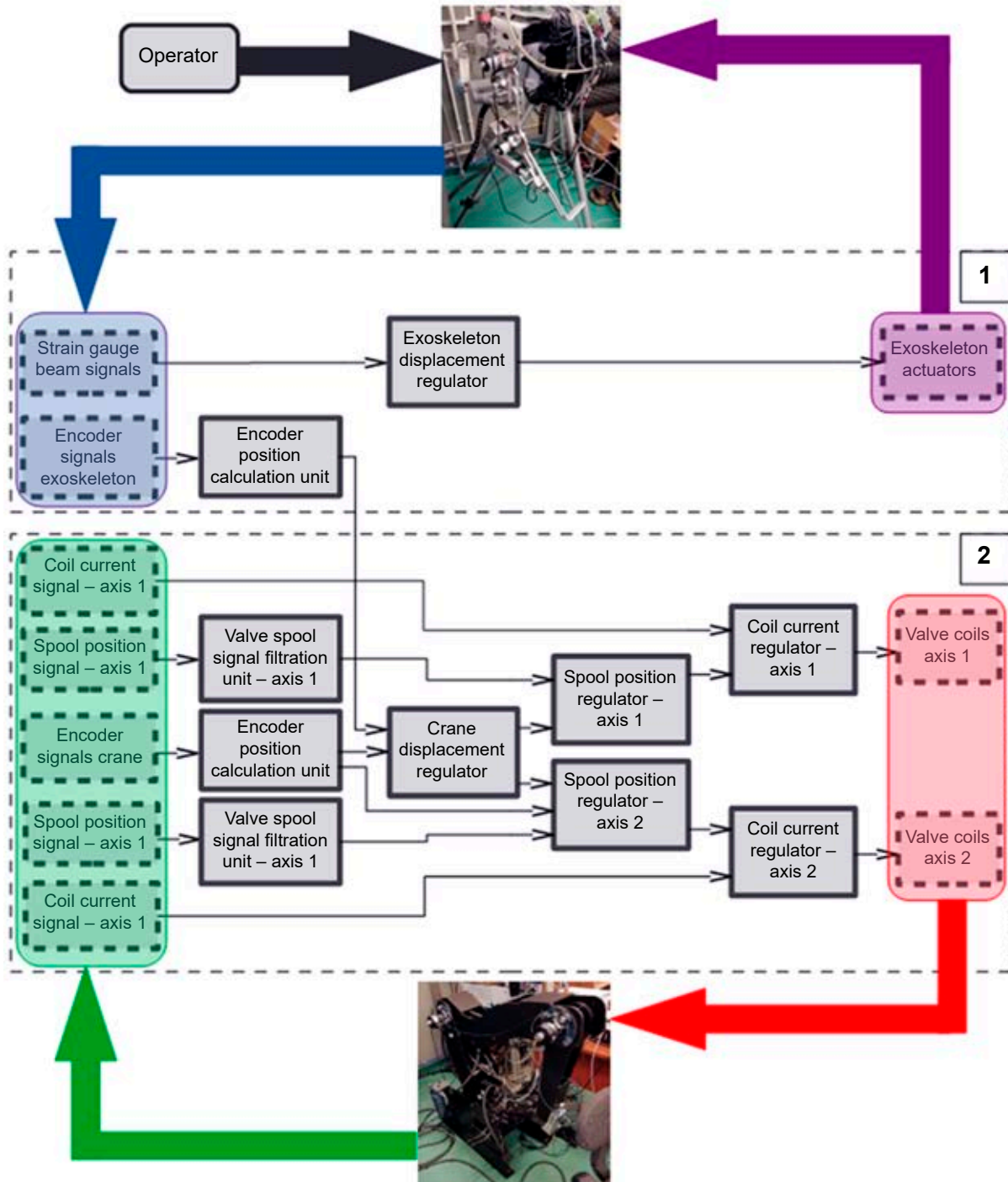


Figure 3. Diagram of the crane control system using an exoskeleton

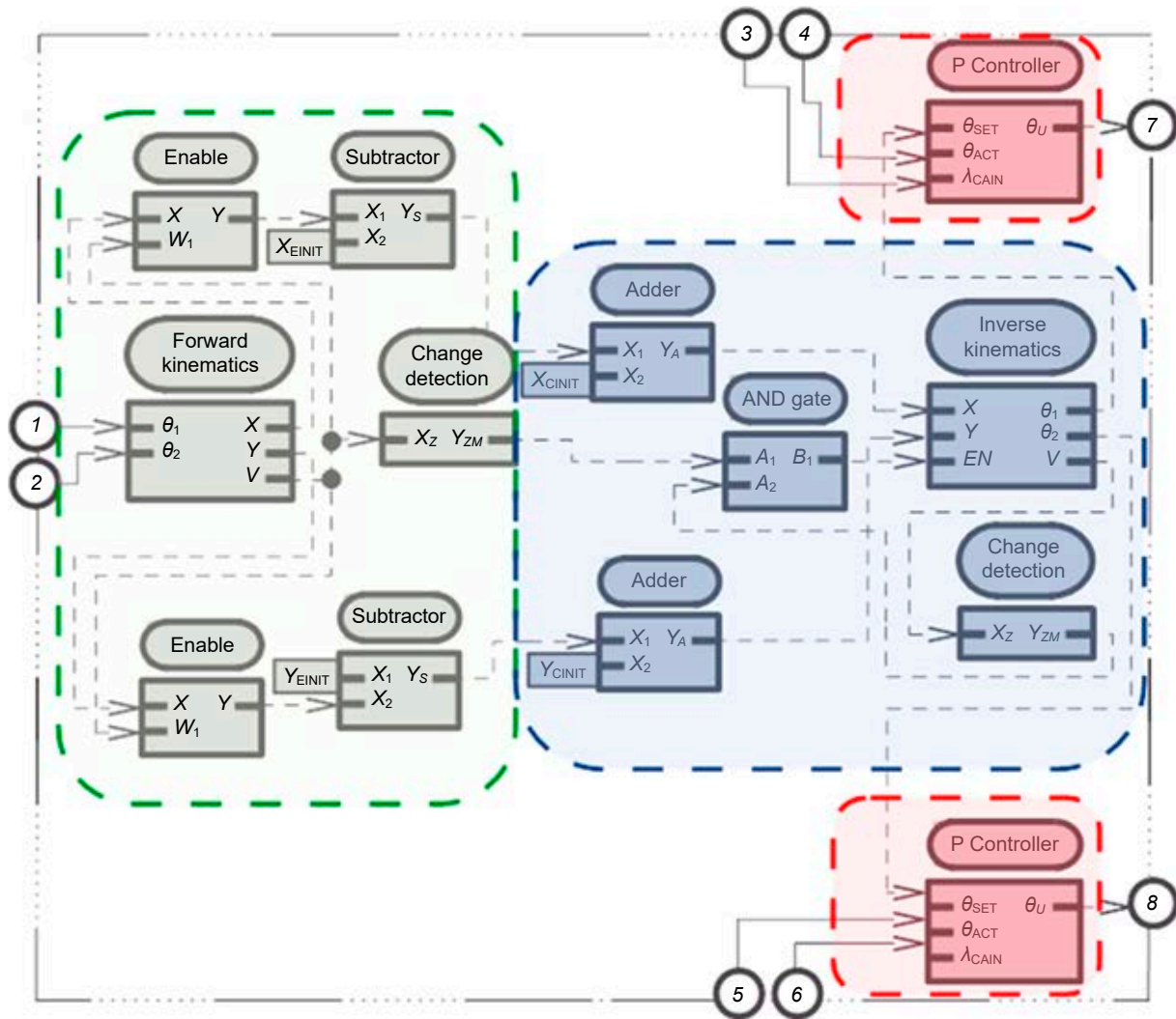


Figure 4. Crane displacement regulator

effector, based on measured exoskeleton angles (Figure 4 – inputs 1, 2). Then, knowing the initial values of the exoskeleton position, the exoskeleton displacement was calculated

- Section for calculating the crane set position (Figure 4 – blue section). Based on the displacement calculated by the previous section and the crane’s initial position, the crane’s set position is determined. Then, using the inverse kinematics equations, the given position of the system in configuration coordinates is calculated.
- Section of proportional regulators (Figure 4 – red section), based on the set and measured (Figure 4 – inputs 4, 5) angular positions of the crane members. Inputs 3 and 6 are P controller gains.

The control values of the crane displacement regulator are then transferred to the valve spool position regulator, which controls the extension speed of the piston rods of the actuators. Analysis of the operation of the valve spool showed that the location

of the spool at a certain positional range causes the crane members to oscillate, which negatively impacts the mechanical parameters of the system (fatigue strength).

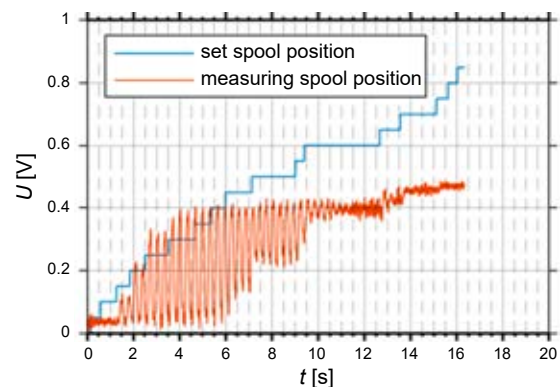


Figure 5. Deadband zone of the spool valve

The regulator consisted of two subsystems: a system to prevent work in the valve dead zones

(an example of the workflow in the dead zone is given in Figure 5), and a converter that converts the set position of the spool into the set coil current for the spool valve coil current regulator. Due to the need to accurately position the valve spool, the converter was based on a proportional-integral regulator with a zero steady-state offset.

The control values of the spool valve positioner were then transferred to the inputs of the spool valve coil current regulator. The controller was based on a proportional controller with forward compression in the form of an inverse coil hysteresis model. The influence of the set signal frequency on the course of the hysteresis curve is shown in Figure 6.

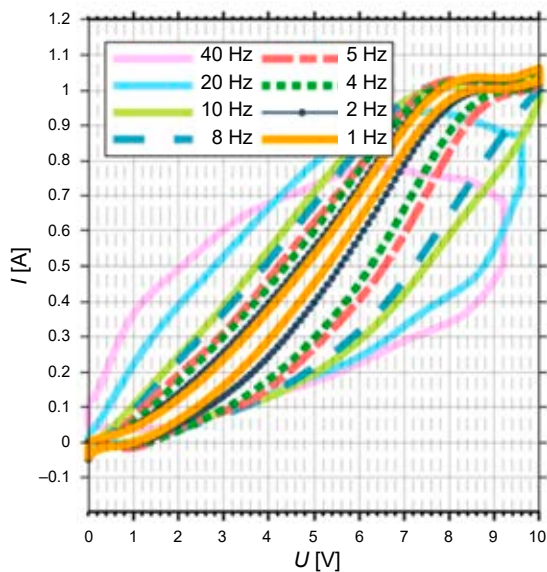


Figure 6. Influence of the frequency of the sinusoidal signal on the hysteresis curve

A hysteresis model for a frequency of 5 Hz was applied because it was assumed that the operator would change the position of the exoskeleton end effector terminal at a frequency lower than 2 Hz. In addition, the following auxiliary units were implemented in the control system:

- A system to calculate the encoder position based on reading and appropriately interpreting rectangular signals generated by measuring pins. The system was also equipped with a protection unit against incorrect pulse counting caused by contact vibrations.
- Filtering system – due to the significant noise of the valve spool position signal, it was necessary to filter it. The filtering system was based on a PPRLN filter (Saków, Parus & Miądlicki, 2017), which has a near-zero phase shift at low operating frequencies.

Control system validation

The last stage was to assess the correct operation of the implemented control system. To this end, the operator started to move the exoskeleton end effector and then observed the crane's behavior. The forces exerted on the exoskeleton joints are shown in Figures 7 and 8.

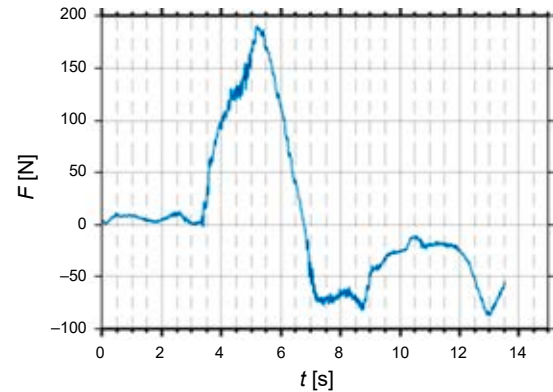


Figure 7. Force from strain gauge beam – joint 1

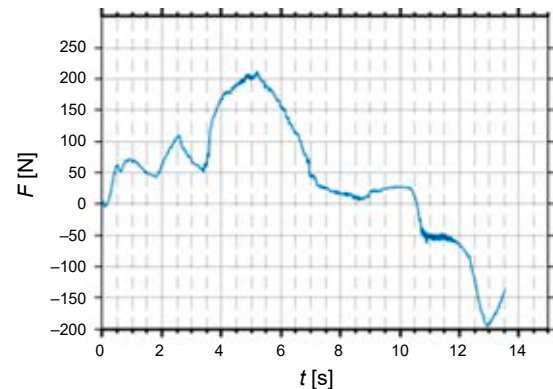


Figure 8. Force from strain gauge beam – joint 2

The angular displacements of the exoskeleton joints caused by the forces generated by the operator are shown in Figures 9 and 10.

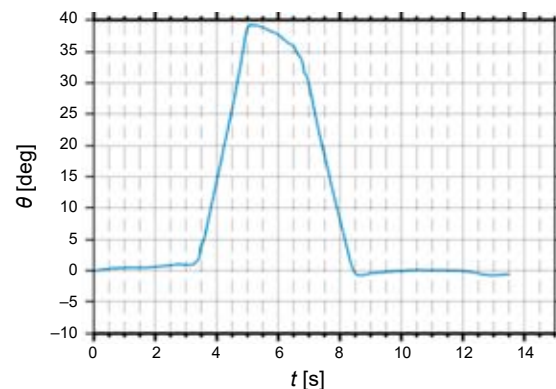


Figure 9. Angle – exoskeleton – joint 1

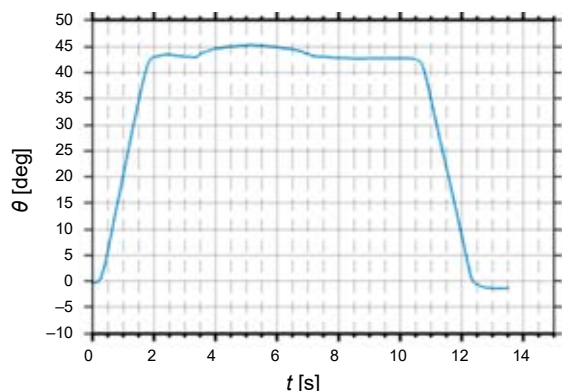


Figure 10. Angle – exoskeleton – joint 2

Based on the current position of the exoskeleton, the set position of the crane was calculated. The set position of crane joints, along with the measured position of crane joints, are shown in Figures 11 and 12.

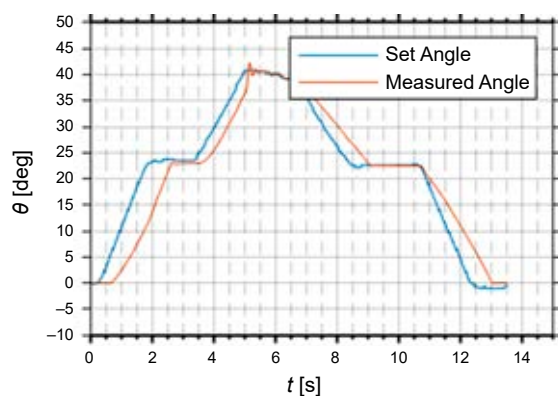


Figure 11. Set and measured angle – crane – joint 1

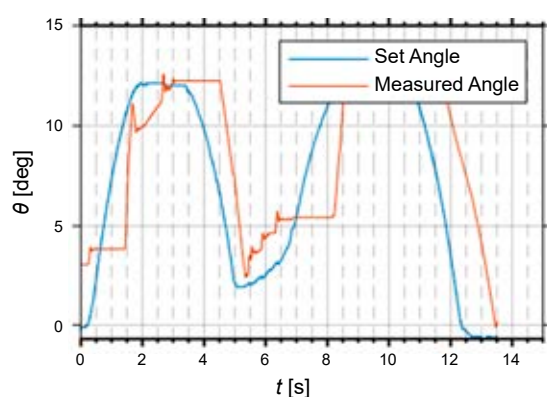


Figure 12. Set and measured angle – crane – joint 2

Conclusions

Analysis of Figures 7–12 showed that the system properly performed its teleoperation task. The maximum steady-state positioning error for joint 1 was

approximately 0.5° and approximately 1° for joint 2. The use of the control system on a programmable system based on the hardware description language made it possible to design an application in which individual units worked in parallel, which significantly reduced delays in the control path. Additionally, by using the VHDL hardware description language, the control system developer had more control over the implementation of individual functions.

References

1. BEJGER, A. & DRZEWIENIECKI, J.B. (2020) A New Method of Identifying the Limit Condition of Injection Pump Wear in Self-Ignition Engines. *Energies* 13, 7, DOI: 10.3390/en13071601.
2. BEJGER, A., CHYBOWSKI, L. & GAWDZIŃSKA, K. (2018) Utilising elastic waves of acoustic emission to assess the condition of spray nozzles in a marine diesel engine. *Journal of Marine Engineering & Technology* 17, 3, pp. 153–159.
3. CHANG, E.H.E., KIM, H.Y., KOH, Y.W & CHUNG, W.Y. (2017) Overview of robotic thyroidectomy. *Gland surgery* 6, 3, pp. 218–228.
4. CHYBOWSKI, L., GAWDZIŃSKA, K., ŚLESICKI, O., PATEJUK, K. & NOWOSAD, G. (2015) An engine room simulator as an educational tool for marine engineers relating to explosion and fire prevention of marine diesel engines. *Scientific Journals of the Maritime University of Szczecin, Zeszyty Naukowe Akademii Morskiej w Szczecinie* 43 (115), pp. 15–21.
5. Elektronika Praktyczna (2004) *Elektronika Praktyczna – Układy programowalne, część 2*. [Online] Available from: <https://ep.com.pl/files/4414.pdf> [Accessed: July 15, 2020].
6. ETHW (2017) *Integrated Circuits*. [Online] Available from: https://ethw.org/Integrated_Circuits [Accessed: July 19, 2020].
7. HERBIN, P. & PAJOR, M. (2018) *The torque control system of exoskeleton ExoArm 7-DOF used in bilateral teleoperation system*. AIP Conference Proceedings, pp. 020020-020020-9.
8. HERBIN, P. & WOŹNIAK, M. (2019) Bilateral teleoperation system for a mini crane. *Scientific Journals of the Maritime University of Szczecin, Zeszyty Naukowe Akademii Morskiej w Szczecinie* 57 (129), pp. 63–69.
9. HOLLIDAY, M., DOUGAN, A., GAVEL, D., GUSTAVESON D., JOHNSON, R., KETTERING, B. & WILHELMSEN, K. (1993) *Demonstration of automated robotic workcell for hazardous waste characterization*. IEEE International Conference on Robotics and Automation, May 2–7, 1993, Atlanta, Georgia, pp. 768–794.
10. HSU, K., MURRAY, C. & COOK, J. (2013) *China's Military Aerial Vehicle Industry*. U.S.-China Economic and Security Review Commission.
11. KAESLIN, H. (2015) *Top-Down Digital VLSI Design*. Elsevier, pp. 41–61.
12. KAWATSUMA, S., FUKUSHIMA, M. & OKADA, T. (2012) *Emergency response by robots to Fukushima Daiichi accident: summary and lessons learned*. Japan Atomic Energy Agency, pp. 428–435.
13. KOZAK, M., GORDON, R. & BEJGER, A. (2016) Control of squirrel-cage electric generators in a parallel intermediate DC circuit connection. *Scientific Journals of the Maritime University of Szczecin, Zeszyty Naukowe Akademii Morskiej w Szczecinie* 45 (117), pp. 17–22.

14. MIĄDLICKI, K. & PAJOR, M. (2015) Overview of user interfaces used in load lifting devices. *International Journal of Scientific and Engineering Research* 6, 9, pp. 1215–1220.
15. NARAYANAN, S. & REDDY, C.R. (2015) Bomb Defusing Robotic Arm using Gesture. *International Journal of Engineering Research & Technology (IJERT)* 4, 2.
16. PAJOR, M., STATECZNY, K., PIETRUSEWICZ, K. & URBAŃSKI, Ł. (2011) Zastosowanie modeli wirtualnych do sterowania obrabiarek. *Modelowanie Inżynierskie*, pp. 311–317.
17. SAKÓW, M., PARUS, A. & MIĄDLICKI, K. (2017) Filtr LS i jego implementacja w sterowniku systemu master-slave z siłowym sprzężeniem zwrotnym. *Modelowanie Inżynierskie* 65, pp. 107–117.
18. SICILIANO, B. & KHATIB, O. (2016) *Springer Handbook of Robotics*. Springer, pp. 1423–1462, 1521–1548, 1552–1558, 1784–1786.